The Influence of the Excitation Intensity on the Laser Spectra of acidified Solutions of 4-Methylumbelliferone

T. KINDT, E. LIPPERT, and W. RAPP

Iwan N. Stranski-Institut für Physikalische und Theoretische Chemie der Technischen Universität Berlin

(Z. Naturforsch. **27 a**, 1371—1373 [1972]; received 14 June 1972)

The influence of the excitation intensity on the laser spectra of solutions of 4-methylumbelliferone in HCl/C_2H_5OH has been investigated. There are three distinct laser emissions at 4100 Å, 4900 Å and 5300 Å, respectively, the third of which only occurs within a HCl-concentration range of 10^{-2} m/l $< c_{HCl} <$ 2.5 m/l. This emission is quenched if the laser threshold for the emission of the neutral form of 4-methylumbelliferone at 4100 Å is exceeded.

Introduction

Changes in the electronic state of a molecule give rise to changes in many of its physical and chemical properties: e. g. excitation of aromatic molecules from the singlet ground state S_0 to the first excited singlet state S_1 leads to an increase in the strength of the basic and acidic groups [1]. This should also apply to the hydroxyl groups as well as to the carbonyl and ring-oxygen atoms of 4-methylumbelliferone (4-MU).

Recent publications have shown that solutions of 4-MU are laser-active [2, 3]. An investigation of laser-pumped acidified ethanolic solutions has indicated that three fluorescent laser-active molecular species are co-existing in the same solution of the dye.

These authors [3] have demonstrated that in acidic solutions the excited neutral form N* of the dye undergoes a fast chemical reaction to form two cations A* and B* of the type $[N^*H]^+$ (proton exciplexes). These excited molecules deactivate by spontaneous or induced emission, or radiationless processes, to unstable ground state cations which rapidly dissociate to give a neutral molecule N and a proton. The latter can be seen from the fact that the absorption spectra are independent of the acid concentration of the dye solution. By carefully adjusting the pH-value of the solution, three distinct laser emissions can be obtained from the same solution which originate from N*, A* and B*. These emissions occur at different wavelengths and are separated from each other by some hundred Angström units (see Figure 1).

This paper deals with the dependence of the intensities of the above mentioned laser emissions on the HCl concentration and the excitation intensity. It has been found that the long-wavelength laser emission of the B* proton exclipex is suppressed:

1) if the B* formation rate is too small due to insufficient proton concentration,
2) if a quenching process originating from the presence of Cl^--ions becomes relevant in strongly acidified solutions,
3) if the threshold of the neutral 4-MU laser is exceeded, using high excitation intensities.

The population density of B* falls below the laser-threshold value and B* laser-emission is not obtainable in all three cases.

Experimental

The dye solutions were pumped using a transversal arrangement. The second harmonic generated output of a *Q*-switched ruby laser was focussed with a cylin-

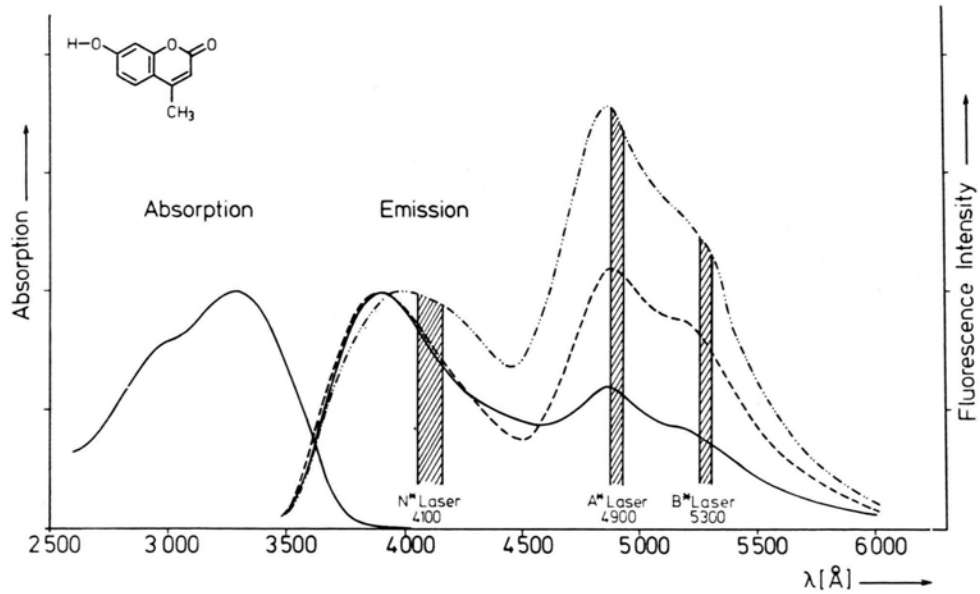

Fig. 1. Absorption and emission spectra of HCl-acidified ethanolic 4-MU solutions ($c_{4\text{-MU}} = 10^{-4}$ m/l, with ——— 0.01 m/l, – – – – 0.1 m/l, —·—·—·— 1 m/l HCl). — The emission spectra were obtained with an excitation wavelength of 3472 Å. The hight of the first peak of the emission spectrum has always been set equal to the absorption peak.

drical lense ($f = 13$ cm) into a 1 cm square quartz cell containing the acidified 4-MU solutions. The maximum output of the ruby laser was 300 MW at 6943 Å, the full half-width of the laser pulses being 15 ns. The dye laser resonator consisted of nothing other than the dye cell in order to obtain identical resonator conditions for all three dye laser emissions.

The dye laser output was recorded with a grating monochromator (Perkin-Elmer, model E1) which was equipped with a Polaroid camera. The film was a Polaroid, type 410.

The ruby laser flashlamp high voltage (in kV) was used as a reference for the excitation intensity. This appeared to be directly proportional to the 6943 Å ruby laser output.

Results

The experimental results are shown in Figs. 2 and 3. The laser emission of neutral 4-MU and of proton exciplex states can be seen at 4100 Å (N*), 4900 Å (A*) and 5300 Å (B*). The laser emission of the B* exciplex state was obtained for solutions with a HCl-concentration ranging between $0.01 \text{ m/l} < C_{HCl} < 2.5 \text{ m/l}$ only (see Figure 2).

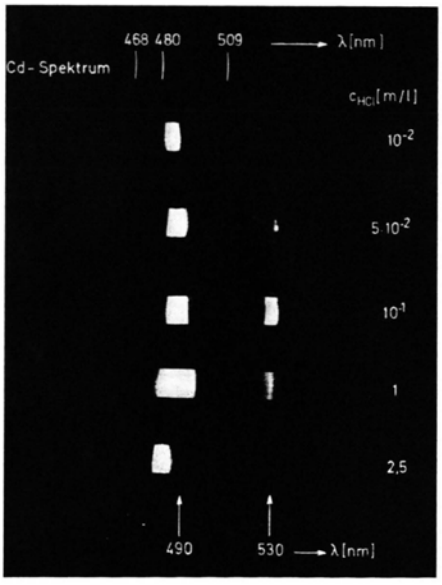

Fig. 2. Laser spectra of different HCl-acidified ethanolic 4-MU solutions above the exciplex laser threshold, $c_{4\text{-MU}} = 5 \times 10^{-2}$ m/l.

The dependence of the laser spectrum of such a solution ($C_{HCl} = 0.1$ m/l) on the excitation intensity is shown in Figure 3. The threshold for B* laser emission and A* laser emission is reached for $U = 6.69$ kV and $U = 6.71$ kV respectively. Both emissions are enhanced by enlarging the excitation intensity. If the threshold value of the neutral 4-MU laser is exceeded at $U = 6.9$ kV, the B* laser emission decreases sharply and disappears at $U = 7$ kV. On the other hand, the intensities of both the N*- and A*-lasers increase by increasing the excitation intensity to the highest pumping intensity obtainable at $U = 7.15$ kV.

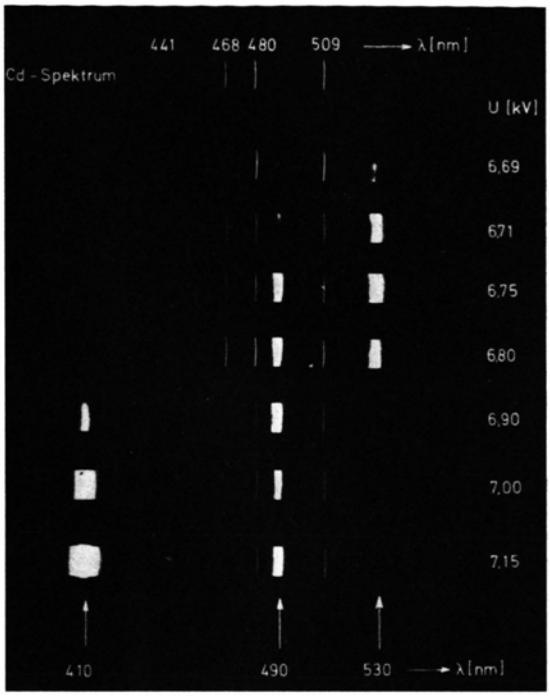

Fig. 3. Dependence of the 4-MU dye laser spectra on the excitation intensity. $c_{4\text{-MU}} = 5 \times 10^{-2}$ m/l, $c_{HCl} = 0.1$ m/l, U = ruby laser flashlamp voltage in kV.

Discussion

Protonation seems to be probable on the two basic groups of the neutral form of 4-MU, i. e. the carbonyl-group or the ring-oxygen:

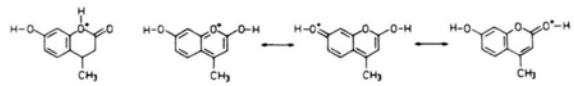

I II

Structure II is most likely the lower energy form owing to the number of contributing mesomeric states.

As to the population of the proton exciplex states A* and B*, two different formation mechanisms seem possible:

1) A parallel reaction $N^* \begin{matrix} \nearrow A^* \\ \searrow B^* \end{matrix}$ corresponding to a direct protonation either on the ring-oxygen atom or on the carbonyl group.
2) A stepwise population $N^* \rightarrow A^* \rightarrow B^*$ corresponding to a protonation followed by a further reaction step which leads to the energetically favourable species B*. This step may be a tautomerisation or a dissociation.

Earlier investigations [3] indicated that the formation rate of the B* proton exciplex is probably slower than that of the A* proton exciplex. This fact would explain the sensitivity of B* laser emission to various processes which compete with the population of the B* state.

On the basis of the experimental facts any one of these processes which have been enumerated below can cause a decrease in the B* population density below the laser threshold value:

1) The formation of A* exciplexes quenching the B* laser emission at low HCl-concentration.
2) A quenching process due to Cl^--ions in strongly acidified solutions leading to radiationless deactivation of both exciplex states A* and B* [4].
3) The laser emission from the state N* of the neutral molecule.

We are now carrying out further investigations in order

1) to identify the structure of the proton exciplex states,
2) to explain the mechanism of the photochemical protonation processes,
3) to explain the mechanism of quenching the B* laser emission if the laser threshold of the neutral 4-MU is exceeded.

We are investigating oxygen-alcylated 4-MU derivates in this context and compare the results of measurements of the 4-MU N*-, A*-, B*-laser intensities, as a function of the excitation intensity, with theoretical dependencies obtainable from the numerical solution of the laser rate-equations associated with different proton exciplex formation mechanisms.

We thank the Deutsche Forschungsgemeinschaft, the Fonds der Chemischen Industrie and the Stifterverband der Deutschen Industrie for financial support.

[1] TH. FÖRSTER, Z. Elektrochem. **54**, (1), 42 [1950].
[2] C. V. SHANK, A. DIENES, A. M. TROZOLLO, and J. A. MYER, Applied Physics Letters **16**, (10), 405 [1970].
[3] A. DIENES, C. V. SHANK, and A. M. TROZOLLO, Appl. Phys. Letters **17**, (5), 189 [1970].
[4] A. BERGMANN, R. DAVID, and J. JORTNER, Opt. Comm. **4**, (6), 431 [1972].

Tunable Stimulated Raman Emission Generated by a Dye Laser

W. SCHMIDT and W. APPT

Carl Zeiss, Forschungsgruppe, 7082 Oberkochen

(Z. Naturforsch. **27 a**, 1373—1375 [1972]; received 26 July 1972)

One well-known method of generating tunable stimulated Raman emission (SRE) makes use of a Raman medium, with a Raman shift varied by an external magnetic field and pumped by a fixed-frequency laser. This method is realized with the spin-flip Raman laser [1].

In this paper we want to discuss a different approach to tunable SRE. The basic idea is to pump an ordinary Raman medium having a fixed Raman shift by a tunable laser. Dye lasers are promising pumping sources because they are capable of generating high powers over a broad tunability range. Powerful flashlamp-pumped dye lasers are made, for instance, from brilliant sulphaflavine (508 – 574 nm) [2], rhodamine 6G (570 – 630 nm) and a mixture of rhodamine 6G and cresyl violet (630 – 710 nm) [3]. They cover a spectral range with a width larger than the Raman shift corresponding to the Q_1 component of the fundamental vibrational transition of hydrogen (4155 cm^{-1}) [4]. As shown by Table 1, the Stokes and anti-Stokes SRE lines up to the 4-th step, generated by these lasers in hydrogen, may together with the dye laser emission cover the entire spectrum from the UV to the far IR. Hydrogen is a favorable medium because of its large Raman shift and because it is to a large extent free from absorption and dispersion in the region of interest.

The feasibility of SRE generation in H_2 by dye laser pumping was investigated in a preliminary experiment. The experimental setup is shown in Figure 1. A 20 mm long dye cell was longitudinally pumped by a passively Q-switched ruby laser. The 400 mm long dye laser cavity consisted of a roof prism and a resonant reflector (LAK 10-flat). From $5 \cdot 10^{-5}$ molar solutions of 3.3′-diethylthiatricarbocyanine bromide (DTTC) in ethanol or in DMSO, output powers up to 85 MW were obtained when pumping pulses of 330 MW peak power and 10 nsec duration were applied. The dye laser emission band was 13 nm wide with its central wavelength at 795 nm (ethanol) or 830 nm (DMSO). For spectral narrowing, interference filters and/or Fabry-Perot-etalons (FPE) were inserted into the cavity. The dye laser beam was focussed by a 200-mm focal length lens into a 300-mm long vessel containing room-temperature hydrogen at a pressure of 200 atmospheres. For power measurements by planar vacuum photocells (ITL), the different SRE beams emerging through an exit window at the oposite end of the vessel were spatially separated by a 3-prism-set. Spectra were recorded on Polaroid film type 47, using a grating spectroscope.

Table 1. Potential tunability ranges.

Wavelength/nm from	to	pumping lasers	
530	679		
679	947	1st	step of Stokes SRE
947	1560	2nd	
1560	4440	3rd	
4440	(∞)	4th	
433	530	1st	step of anti-Stokes SRE
368	433	2nd	
319	368	3rd	
282	319	4th	

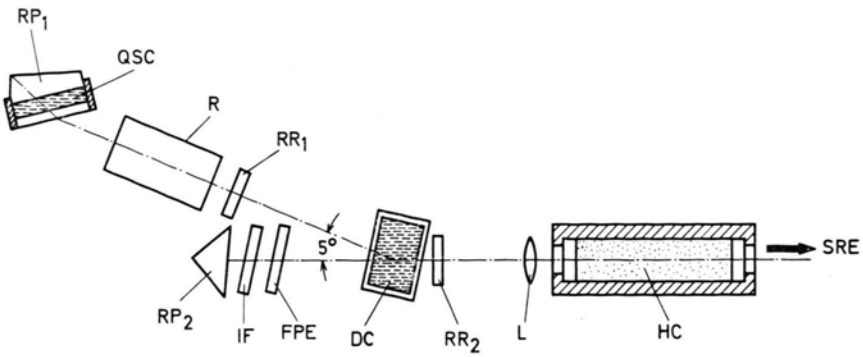

Fig. 1. The experimental setup.
R: ruby-laser head; RP_1: roof prism;
OSC: Q-switch dye cell;
RR: resonant reflector.
DC: dye-laser cell, RP_2: roof prism;
IF: interference filter;
FPE: Fabry-Perot-etalon;
RR: resonant reflector; L: lens;
HC: hydrogen cell.

85 MW of broadband, nonpolarized dye laser power, i. e. a spectral power density of 6.5 MW/nm, were not sufficient to excite SRE. When, however, the bandwidth was reduced to 3 nm using an intracavity interference filter (Fig. 2 b), which reduced the power to 58 MW but increased the spectral power density to about 19 MW/nm, bright 1-st and 2-nd anti-Stokes SRE was observed. The laser was tuned by tilting the interference filter. The tunability range within which the dye laser power exceeded the SRE threshold was found to be 7 nm, centered at 826 nm. Figure 2 c shows a SRE spectrum with the first anti-Stokes line at 612 nm and the second anti-Stokes line at 487 nm.

In further experiments the spectral density of the pumping radiation was increased by employing 1-mm, 0.25-mm, 0.15-mm and 0.05-mm thick FPE's, coated with 60% reflecting dielectric mirrors. This resulted in multiple-line spectra with up to 20 lines, and line widths between 0.2 and 0.01 nm. Combining the interference filter used to obtain Figs. 1 b and 1 d with a 0.05-mm thick FPE resulted in two lines each about 0.2 nm wide. In all cases SRE was observed. Figures 1 e and 1 f show the dye laser spectra obtained with a 0.05-mm FPE and the corresponding anti-Stokes lines. The individual lines of each spectrum are separated by $\Delta\lambda = \lambda^2/2\,n\,t$, where λ is the wavelength of the dye laser or Raman emission and $n\,t = 0.075$ mm is the optical thickness of the FPE. In this case tuning was achieved by changing the solvent.

A certain instability of SRE output was probably caused by variations in the transverse mode structure [5] of the dye laser from shot to shot and by increasing damage in the ruby. Therefore, reliable power measurements were difficult. With dye laser powers between 45 and 60 MW, and with a 0.05-mm FPE inside the dye laser cavity, the 1-st anti-Stokes powers ranged from 0 to 125 kW, the 2-nd anti-Stokes powers from 0 to 2 kW. The first Stokes line was registered as a burn mark on exposed polaroid at a wavelength of 1.2 microns. The 2-nd Stokes line (2.6 microns) was not expected to be observed because we used glass optics.

With the present setup the pump powers to obtain SRE were inconveniently high. Our attempts to drastically reduce the SRE threshold and to increase the tunability range will include the construction of high-power, narrow-band, mode-controlled dye lasers, which are pumped by flashlamps. We will also provide an appropriate resonant cavity for the Raman laser and test some other promising Raman media.

We acknowledge valuable discussions with Dr. M. MAIER and Prof. Dr. F. P. SCHÄFER. The work upon which this report is based, was supported by the Bundesminister für Bildung und Wissenschaft as part of his technology program. Solely the authors are responsible for the contents of this report.

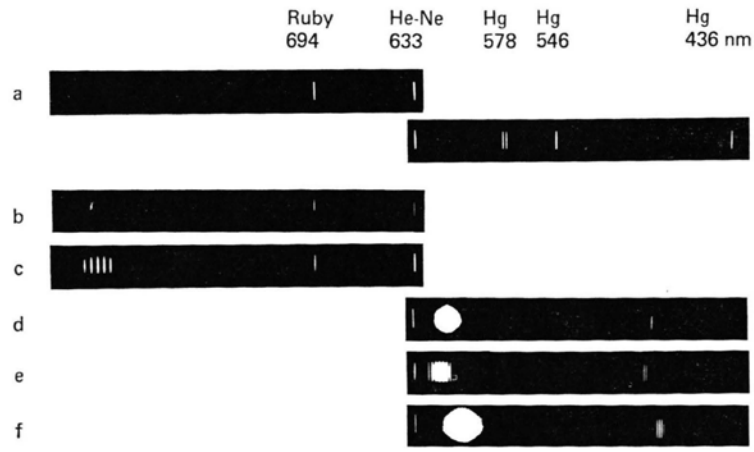

Fig. 2. a) Reference lines; b) dye laser emission at 830 nm, narrowed by an interference filter (FWHM = 11 nm, maximum transmission 95%) inside the cavity; c) multiple-line dye laser spectrum obtained with a 0.05-mm thick quartz FPE with dielectric coatings (60% reflection) inside the cavity; d) 1st and 2nd anti-Stokes lines generated by the dye laser with interference filter inside the cavity; e), f) anti-Stokes lines generated by the multiple-line dye laser. – The DTTC was dissolved in DMSO (a to e) and in ethanol (f). Because of the film sensitivity relative intensities cannot be judged from the spectra. Some of the lines are broadened by strong overexposure.

* *Note added in proof:* After completion of the manuscript, it was brought to our attention that tunable Raman emission was generated, using a neodym laser tuable within a range of 200 cm^{-1} and pyridine as a Raman medium. R. V. AMBARTSUMYAN, V. M. APATIN, and V. S. LETOKHOV, JETP Letters **15**, (6), 237 [1972].

[1] C. K. N. PATEL and E. D. SHAW, Phys. Rev. Lett. **24**, 451 [1970].

[2] J. B. MARLING, D. W. GREGG, and L. WOOD, Appl. Phys. Lett. **17**, 527 [1970].

[3] W. SCHMIDT, W. APPT, and N. WITTEKINDT, Z. Naturforsch. **27 a**, 34 [1972].

[4] R. W. MINCK, R. W. TERHUNE, and W. G. RADO, Appl. Phys. Lett. **3**, 181 [1963].

[5] N. BLOEMBERGEN and Y. R. SHEN, Phys. Rev. Lett. **13**, 720 [1964].

Inkohärente Lichtstreuung an Ladungsdichteschwankungen schwach ionisierter Plasmen in Magnetfeldern

G. KLINGENBERG und E. W. RICHTER

Lehrstuhl B für Theoretische Physik
Technische Universität Braunschweig

(Z. Naturforsch. **27 a**, 1375—1376 [1972]; eingegangen am 9. Juni 1972)

Incoherent Scattering of Light from Charge-Density Fluctuations in Weakly Ionized Magnetoplasmas

The spectral density of light scattering from weakly ionized plasmas embedded in a homogeneous magnetic field $\boldsymbol{B}$ is given by the work of WILLIAMS and CHAPPELL [1, 2] and KLINGENBERG [3]. The spectral density has been computed for electron plasmas and is analyzed for the case $\boldsymbol{k} \perp \boldsymbol{B}$ ($\boldsymbol{k}$ is the difference between the wave vectors of the incident wave and the scattered wave) in the regimes $k D \gg 1$ and $k D \ll 1$ (D is the Debye length).

Wird ein Plasma durch eine monochromatische elektrische Welle (Laser) angeregt, so entsteht eine Streustrahlung, deren spektrale Intensität gemessen werden kann.

WILLIAMS und CHAPPELL [1, 2] und KLINGENBERG [3] betrachten ein Dreikomponentenplasma, in dem die Stöße zwischen geladenen und neutralen Teilchen durch einen BGK-Ansatz [4] beschrieben werden. Aus den Zweiteilchen-Korrelationsfunktionen läßt sich die spektrale Dichte $S(\boldsymbol{k}, \omega)$ der Streustrahlung berechnen:

$$S(\boldsymbol{k}, \omega) = -\frac{2(kD)^2}{\omega} \operatorname{Re} \frac{i(1-B_i/F_i)\, B_e/F_e}{1-B_i/F_i-B_e/F_e} \qquad (1)$$

$\omega = \omega_2 - \omega_1$ und $\boldsymbol{k} = \boldsymbol{k}_2 - \boldsymbol{k}_1$ bezeichnen die Differenzen der Frequenzen und Wellenzahlvektoren von einfallender $(\omega_1; \boldsymbol{k}_1)$ und gestreuter $(\omega_2; \boldsymbol{k}_2)$ Welle; D ist die Debye-Länge. Die Größen B_e, F_e bzw. B_i, F_i lassen sich auf einfachere Integrale K_e bzw. K_i zurückführen:

$$B_e = -\frac{1}{(kD)^2}\,(F_e + i\,\omega\,K_e)\,; \qquad (2\,a)$$

$$B_i = -\frac{1}{(kD)^2}\,(F_i + i\,\omega\,K_i) \qquad (2\,b)$$

$$F_e = 1 - \nu_{e0}\,K_e\,; \qquad F_i = 1 - \nu_{i0}\,K_i \qquad (3\,a, b)$$

ν_{e0} bzw ν_{i0} sind die Stoßfrequenzen der Elektronen bzw. Ionen mit den Neutralteilchen.

Die Integrale K_e und K_i sind in einer für numerische Auswertungen zweckmäßigen Form darstellbar (KLINGENBERG [3]):

$$K_e = \lim_{s \to -i\omega} \sum_{n=-\infty}^{\infty} X_{ne} \int_{-\infty}^{-\infty} du\, \frac{f_e(u)}{s + i\,k\,u\cos\Theta + \nu_{e0} + i\,n\,\omega_c}\,, \qquad (4\,a)$$

$$K_i = \lim_{s \to -i\omega} \sum_{n=-\infty}^{\infty} X_{ni} \int_{\infty}^{\infty} du\, \frac{f_i(u)}{s + i\,k\,u\cos\Theta + \nu_{i0} + i\,n\,\Omega_c}\,. \qquad (4\,b)$$

In (4) bezeichnet s eine komplexe Variable; ω_c bzw. Ω_c die Gyrofrequenz der Elektronen bzw. Ionen; Θ den Winkel zwischen dem Wellenzahlvektor $\boldsymbol{k}$ und der Richtung des äußeren Magnetfeldes $\boldsymbol{B}$; f_e bzw. f_i die eindimensionale Maxwell-Geschwindigkeitsverteilungsfunktion der Elektronen bzw. Ionen. In den Größen X_{ne} bzw. X_{ni} treten modifizierte Bessel-Funktionen $I_n(\lambda)$ erster Art der Ordnung n auf:

$$X_{ne} = \exp\left\{-\frac{k^2 v_e^2 \sin^2\Theta}{\omega_c^2}\right\} I_n\left(\frac{k^2 v_e^2 \sin^2\Theta}{\omega_c^2}\right); \qquad (5\,a)$$

$$X_{ni} = \exp\left\{-\frac{k^2 v_i^2 \sin^2\Theta}{\Omega_c^2}\right\} I_n\left(\frac{k^2 v_i^2 \sin^2\Theta}{\Omega_c^2}\right). \qquad (5\,b)$$

v_e bzw. v_i ist die thermische Geschwindigkeit eines Elektrons bzw. Ions.

Im Grenzfall verschwindender Stoßfrequenzen ν_{e0}, ν_{i0} ergibt sich mit (2) bis (5) aus (1) das Ergebnis von SALPETER [5] [Gl. (17)].

Im folgenden diskutieren wir nur jenen Teil des Streuspektrums, für den allein die Elektronenbewegung wesentlich ist, d. h. $\omega \gg k\,v_i$ und $\omega \gg \Omega_c$. Dann gilt $B_i/F_i = 0$ und (1) vereinfacht sich zu

$$S(\boldsymbol{k}, \omega) = \frac{2(kD)^2}{\omega} \frac{\varepsilon_i(\boldsymbol{k}, \omega)}{\varepsilon_r^2(\boldsymbol{k}, \omega) + \varepsilon_i^2(\boldsymbol{k}, \omega)}\,, \qquad (6)$$

wobei für die Dielektrizitätskonstante ε_L (Index L kennzeichnet, daß nur Raumladungsschwankungen berücksichtigt wurden) gilt

$$\varepsilon_L = \varepsilon_r + i\,\varepsilon_i = 1 - (B_e/F_e)\,. \qquad (7)$$

Die Maxima der Spektrallinien liegen für $|\varepsilon_i| \ll |\varepsilon_r|$ bei Frequenzen $\omega = \omega_M$, die sich als Lösungen der Dispersionsgleichung $\varepsilon_r(\boldsymbol{k}, \omega) = 0$ ergeben.

In der Umgebung von $\omega = \omega_M$ liefert (6) für jeden Wert von $\boldsymbol{k}$ ein Lorentz-Profil

$$S(\boldsymbol{k}, \omega) = \frac{2(kD)^2}{\omega_M\, \varepsilon_r'|_\omega} \frac{A(\boldsymbol{k}, \omega_M)}{(\omega - \omega_M)^2 + A^2(\boldsymbol{k}, \omega_M)} \qquad (8)$$

mit der Linienbreite

$$A(\boldsymbol{k}, \omega_M) = \frac{\varepsilon_i}{\varepsilon_r'}\Big|_{\omega_M}; \qquad \varepsilon_r' = \frac{d\varepsilon_r}{d\omega}. \tag{9}$$

Wird über einen Frequenzbereich $\Delta\omega$ in der Umgebung von ω_M integriert und gilt $\Delta\omega \gg A$, so folgt für die integrierte spektrale Dichte einer Linie:

$$P(\boldsymbol{k}, \omega_M) = 2\pi \frac{(kD)^2}{\omega_M \varepsilon_r'|_{\omega_M}}. \tag{10}$$

Besonders interessant ist das Streuspektrum für den Fall $\boldsymbol{k} \perp \boldsymbol{B}$ ($\Theta = \pi/2$), da sich wegen der verschwindenden Landau-Dämpfung ohne Berücksichtigung von Teilchenstößen δ-förmige Spektrallinien ergeben (vgl. SALPETER [5]). Für $\boldsymbol{k} \perp \boldsymbol{B}$ folgt mit $\lambda = k^2 v_e^2/\omega_c^2$ für die Integrale (2) und (3)

$$B_e = -\frac{1}{\lambda}\frac{\omega_p^2}{\omega_c^2}\left(1 + \sum_{n=-\infty}^{\infty} X_{ne}\frac{\omega + i\nu_{e0}}{n\omega_c - (\omega + i\nu_{e0})}\right)$$
$$= \frac{2}{\lambda}\frac{\omega_p^2}{\omega_c^2}\sum_{n=1}^{\infty}\frac{n^2\omega_c^2}{(\omega + i\nu_{e0})^2 - n^2\omega_c^2} X_{ne}, \tag{11}$$

$$F_e = 1 - i\nu_{e0}\sum_{n=-\infty}^{\infty} X_{ne}\frac{1}{\omega + i\nu_{e0} - n\omega_c} \tag{12}$$

und mit Hilfe von (7)

$$\varepsilon_L = 1 - \frac{\omega_p^2}{\omega_c^2}\sum_{n=1}^{\infty}\frac{X_{ne}}{\frac{\lambda}{2}\left[\left(\frac{\omega + i\nu_{e0}}{n\omega_c}\right)^2 - 1\right]} \cdot \frac{1}{1 - i\nu_{e0}\sum_{n=-\infty}^{\infty} X_{ne}\frac{1}{\omega + i\nu_{e0} - n\omega_c}}. \tag{13}$$

Aus (6) ergibt sich mit (13) die spektrale Dichte im Fall ruhender Ionen und $\boldsymbol{k} \perp \boldsymbol{B}$. Für die beobachtbaren Extremfälle $k \gg D^{-1}$ bzw. $k \ll D^{-1}$ ist die individuelle bzw. kollektive Bewegung der Elektronen wesentlich. In diesen Fällen läßt sich die spektrale Dichte weiter vereinfachen.

a) Wird angenommen, daß die Gyrofrequenz ω_c nicht um eine oder mehrere Größenordnungen größer ist als die Plasmafrequenz ω_p, so folgt aus der Bedingung für den individuellen Bereich $kD \gg 1$ auch $\lambda = [(k^2 v_e^2)/\omega_c^2] \gg 1$. Dann ist eine asymptotische Entwicklung der Bessel-Funktion $I_n(\lambda)$ und damit der Größe $X_{ne}(\lambda)$ möglich. In niedrigster Näherung folgt $I_n(\lambda) = (2\pi\lambda)^{-1/2} e^{\lambda}$ und eingesetzt in (13) ergibt sich für (6):

$$S(\boldsymbol{k}, \omega) = \sqrt{\frac{2}{\pi}}\frac{\omega_c}{k v_e}\sum_{n=-\infty}^{\infty}\frac{\nu_{e0}}{(\omega - n\omega_c)^2 + \nu_{e0}^2}. \tag{14}$$

Das Spektrum besteht also aus unendlich vielen Lorentz-Linien, deren Breite gleich der Stoßfrequenz ν_{e0} ist. Alle Linien liegen bei Vielfachen der Gyrofrequenz ω_c. In dieser Näherung ist die Intensität aller Linien gleich; sie ist proportional zu $\omega_c/k v_e$, also zur Magnetfeldstärke B und zur Wurzel der reziproken Temperatur $1/T$.

b) Ist das äußere Magnetfeld $\boldsymbol{B}$ so stark, daß die Gyrofrequenz ω_c nicht um eine oder mehrere Größenordnungen kleiner ist als die Plasmafrequenz ω_p, so folgt $\lambda \ll 1$ aus der Näherung für den kollektiven Bereich $kD \ll 1$. Die Reihenentwicklung ergibt, wenn bis zu Gliedern in λ^2 entwickelt wird:

$$X_{0e} = 1 - \lambda + \tfrac{3}{4}\lambda^2; \quad X_{1e} = \frac{\lambda}{2} - \frac{\lambda^2}{2}; \tag{15 a}$$

$$X_{2e} = \frac{\lambda^2}{8}; \quad X_{ne} = 0 \ (n > 2) \tag{15 b}$$

Damit folgt aus (13), wenn nur lineare Glieder in λ berücksichtigt werden:

$$\varepsilon_L(\boldsymbol{k}, \omega) = 1 - \omega_p^2\frac{\omega + i\nu_{e0}}{\omega}\left\{\frac{1-\lambda}{(\omega + i\nu_{e0})^2 - \omega_c^2}\right. + \frac{\lambda}{(\omega + i\nu_{e0})^2 - 4\omega_c^2} + \frac{i\nu_{e0}}{\omega}\left.\frac{\lambda\omega_c^2}{[(\omega + i\nu_{e0})^2 - \omega_c^2]^2}\right\}. \tag{16}$$

Diese in λ lineare Näherung gibt nicht das Ergebnis von PLATZMAN, WOLFF und TZOAR [6] wieder. In nullter Näherung ergibt sich

$$\varepsilon_L(\omega) = 1 - \frac{\omega + i\nu_{e0}}{\omega}\frac{\omega_p^2}{(\omega + i\nu_{e0})^2 - \omega_c^2} \tag{17}$$

in Übereinstimmung mit dem Ergebnis von Platzman, Wolff und Tzoar. Die Frequenz der Linienmaxima folgt aus Gl. (17) durch $\varepsilon_r = 0$. Wird für die Stoßfrequenz $\nu_{e0} \ll \omega_c, \omega_p$ vorausgesetzt, so besteht das Spektrum [da (17) nur in nullter Näherung in λ gilt] aus nur zwei Linien $\omega_2 - \omega_1 = \pm\omega_M$ bei der oberen Hybridfrequenz $\omega_M = \sqrt{\omega_p^2 + \omega_c^2}$. Aus Gl. (9) folgt für die Linienbreite

$$A(\omega_M) = \frac{\nu_{e0}}{2}\frac{\omega_p^2 + 2\omega_c^2}{\omega_p^2 + \omega_c^2} \tag{18}$$

und für die integrierte spektrale Dichte nach (10)

$$P(k, \omega_M) = \pi(kD)^2\frac{\omega_p^2}{\omega_p^2 + \omega_c^2} = \pi\lambda\frac{\omega_c^2}{\omega_p^2 + \omega_c^2} \tag{19}$$

Wie man sieht, geht die Intensität dieser Spektrallinie nach Null für $\lambda \to 0$.

[1] R. H. WILLIAMS u. W. R. CHAPPELL, Phys. Fluids **14**, 591 [1971].

[2] W. R. CHAPPELL u. R. H. WILLIAMS, Phys. Fluids **14**, 1938 [1971].

[3] G. KLINGENBERG, Inkohärente Lichtstreuung an Dichteschwankungen schwach ionisierter Plasmen in Magnetfeldern; Diplomarbeit, Techn. Universität Braunschweig 1971.

[4] P. L. BHATNAGAR, E. P. GROSS u. M. KROOK, Phys. Rev. **94**, 511 [1954].

[5] E. E. SALPETER, Phys. Rev. **122**, 1663 [1961].

[6] P. M. PLATZMAN, P. A. WOLFF u. N. TZOAR, Phys. Rev. **174**, 489 [1968].